4136–4150 *Nucleic Acids Research, 2011, Vol. 39, No. 10* *Published online 2 February 2011*
doi:10.1093/nar/gkq1334

Hmo1 directs pre-initiation complex assembly to an appropriate site on its target gene promoters by masking a nucleosome-free region

Koji Kasahara*, Yoshifumi Ohyama and Tetsuro Kokubo

Division of Molecular and Cellular Biology, Graduate School of Nanobioscience, Yokohama City University, Yokohama, 230-0045, Japan

Received August 3, 2010; Revised and Accepted December 16, 2010

ABSTRACT

Saccharomyces cerevisiae **Hmo1 binds to the promoters of ~70% of ribosomal protein genes (RPGs) at high occupancy, but is observed at lower occupancy on the remaining RPG promoters. In *Δhmo1* cells, the transcription start site (TSS) of the Hmo1-enriched *RPS5* promoter shifted upstream, while the TSS of the Hmo1-limited *RPL10* promoter did not shift. Analyses of chimeric *RPS5*/*RPL10* promoters revealed a region between the *RPS5* upstream activating sequence (UAS) and core promoter, termed the intervening region (IVR), responsible for strong Hmo1 binding and an upstream TSS shift in *Δhmo1* cells. Chromatin immunoprecipitation analyses showed that the *RPS5*-IVR resides within a nucleosome-free region and that pre-initiation complex (PIC) assembly occurs at a site between the IVR and a nucleosome overlapping the TSS (+1 nucleosome). The PIC assembly site was shifted upstream in *Δhmo1* cells on this promoter, indicating that Hmo1 normally masks the *RPS5*-IVR to prevent PIC assembly at inappropriate site(s). This novel mechanism ensures accurate transcriptional initiation by delineating the 5′- and 3′-boundaries of the PIC assembly zone.**

INTRODUCTION

In *Saccharomyces cerevisiae*, 138 ribosomal protein genes (RPGs) encode 79 ribosomal proteins (RPs). RPG transcription constitutes ~50% of RNA polymerase II (Pol II)-mediated transcription in rapidly growing cells (1) and consumes an enormous amount of energy and protein resources. RPs are found in equimolar amounts in ribosomes, and their production is coordinately regulated in response to certain environmental conditions, mainly at the transcriptional stage.

During the past 10 years, increasing numbers of factors and/or mechanisms that regulate RPG transcription have been identified. Rap1, the most extensively characterized RPG regulator, binds to most RPG promoters (2,3) and activates transcription by recruiting the NuA4 histone acetyltransferase (HAT) complex and/or TFIID (4–6). Rap1 regulates transcription by forming a nucleosome-free region (NFR) in its target promoters (7–9). Abf1, which binds to fewer RPG promoters, is thought to function similarly to Rap1 in forming NFRs (10), although it is unknown whether Abf1 recruits TFIID and NuA4. Fhl1 also binds to many RPG promoters and recruits the coactivator, Ifh1, or the corepressor, Crf1, in response to environmental stimuli (11–14). Sfp1 regulates RPG transcription and expression of the ribosome biogenesis (*Ribi*) regulon (15,16) via its translocation between nucleus and cytoplasm in response to certain environmental stresses (17); however, its exact function remains unclear.

Hmo1, a high mobility group B (HMGB) protein, plays roles in Pol I and Pol II transcription, rRNA processing, DNA repair and chromosome/plasmid stability (2,18–25). Previous studies showed that Hmo1 binds to the promoter and coding regions of the 35S rRNA gene in a Pol I-dependent manner (2,20,22,26,27). Hmol binds to ~70% of RPG promoters, compared to Rap1 (93%) and Fhl1 (90%), and promotes Fhl1 binding to a subset of RPG promoters. Given that Hmo1 commonly targets both rDNA and RPGs, which are transcribed by two different RNA polymerases (Pol I and Pol II, respectively), one can speculate that it plays a crucial and specialized role in coordinating the transcriptional regulation and synthesis of ribosomes. However, little is known about the molecular function of Hmo1 at either Pol I or Pol II loci. The deletion of *HMO1* (*Δhmo1*) has a milder effect on RPG expression than *Δfhl1* (13), or mutating the Rap1

*To whom correspondence should be addressed. Tel: +81 3 5477 2536; Fax: +81 3 5477 2536; Email: k4kasaha@nodai.ac.jp

binding site (28,29). Furthermore, *Δhmo1* produces different effects among RPGs, which do not necessarily correlate with the amount of Hmo1 binding, suggesting that the primary role of Hmo1 on RPGs may not be transcriptional activation.

In our previous study, we found that *Δhmo1* caused an upstream shift in the transcriptional start site (TSS) of Hmo1-enriched RPG promoters and rescued the growth defects of certain *sua7* (TFIIB) mutants, which, themselves, caused a downstream TSS shift (23). Such suppression phenotypes for *sua*7, which probably depend on a TSS shift in the direction opposite to that of *sua7*, have been found only with mutations in four polypeptides within the pre-initiation complex (PIC): the Tfg1 and Tfg2 subunits of TFIIF (30–33), and the Rpb2 and Rpb9 subunits of Pol II (34–37). Recent studies using a cross-linking technique demonstrated that multiple interactions between TFIIF and Rpb2, which may be reinforced by Rpb9, are critical for TSS selection (38,39). Presumably, mutations that affect these interactions may impair the specific function of Pol II that is required for selecting the appropriate TSS, or for stabilizing RNA–DNA hybrids during initiation, leading to an upstream TSS shift (30,38,39). In contrast to TFIIF, a direct interaction between Pol II and Hmo1 has not been observed (our unpublished data). Furthermore, in *Δhmo1* cells, a TSS shift was only observed at Hmo1-enriched RPGs, while in *tfg1*, *tfg2*, *rpb2* and *Δrpb9* cells, a TSS shift was observed for most class II (Pol II-driven) genes, regardless of Hmo1 binding (30,37). Therefore, we suppose that the upstream TSS shift in *Δhmo1* is caused by a different mechanism than in other mutants, and reflects a defect in a specialized function(s) of Hmo1 with respect to the regulation of transcriptional initiation at the RPG promoter.

The aim of this study was to unveil such a mechanism by determining how *Δhmo1* induces an upstream TSS shift in Hmo1-enriched RPG promoters. From the results of extensive chromatin immunoprecipitation (ChIP) and primer extension analyses, we identified the IVR (intervening region) between the upstream activating sequence (UAS) and the core promoter (Core) of *RPS5* as the binding site of Hmo1, and found that the IVR is nucleosome depleted. In wild-type (WT) cells, the PIC assembled at a site between the IVR and a nucleosome overlapping the TSS (+1 nucleosome), while it assembled within the IVR in *Δhmo1* cells. These results strongly suggested that Hmo1 and +1 nucleosome determine the 5′- and 3′-boundaries, respectively, of a zone available for PIC assembly, thereby directing PIC assembly at a biologically relevant site.

MATERIALS AND METHODS

Yeast strains and plasmids

Standard techniques were used for the growth and transformation of yeast (40). The yeast strains used in this study are listed in Supplementary Table S1. Detailed information for each strain is described in the Supplementary Data. The yeast culture conditions for each experiment are described in the figure legends. The detailed protocol used to construct the plasmids in this study is described in Supplementary Data. Oligonucleotides used in this study are listed in Supplementary Table S2.

Primer extension analysis

Transcription start sites were mapped by primer extension analysis as described previously (23). The primers used were TK3212 (*RPS5*), TK3214 (*ADH1*), TK9589 (*RPL27B*), TK9911 (*RPS5-mini-CLN2*) and TK10595 (*ADE2-C* reporter). Electrophoretic images were acquired by exposing gels to imaging plates (BAS2500, Fuji Film), and the scanning of each lane was carried out using Multi Gauge version 3.0 software (Fuji Film).

ChIP and sequential ChIP analysis

ChIP analysis was conducted according to the Hahn laboratory protocol (http://labs.fhcrc.org/hahn/Methods/mol_bio_meth/hahnlab_ChIP_method.html) with minor modifications. Briefly, DNA was fragmented by sonication to an average size of 400–500 bp for standard ChIP or 100–200 bp for high-resolution ChIP. Immunoprecipitation was conducted using Dynabeads Protein G (Invitrogen) and monoclonal antibodies against FLAG (Sigma-Aldrich; M2), Pk (AbD Serotec; SV5-Pk1) and Myc (Santa Cruz; 9E10); or polyclonal antibodies against histone H3 (Abcam; ab1791), Rap1 (Santa Cruz; yC-19) and Sua7 (in this study, raised against full-length recombinant Sua7 in rabbit). Real-time quantitative PCR analyses were performed using a KAPA SYBR Fast qPCR kit (KAPA) and Mx3000P (Agilent Technologies). PCR conditions were: 95°C for 40 s; 40 cycles of 95°C for 10 s, 52°C for 30 s and 72°C for 10 s. Each experiment was conducted in triplicate and the average and SD for the ratio of immunoprecipitated DNA versus input DNA (IP/input) was calculated. The positions of amplified regions are depicted in each figure. The primer pairs used for PCR are described in the Supplementary Data.

For sequential ChIP analysis, the first immunoprecipitation was performed as for standard ChIP analysis, except that 5 μg of anti-FLAG antibody and cell extracts containing 5 mg of protein were used. After a final wash with TE, precipitates were eluted by incubating beads with 50 μl of ChIP lysis buffer containing 3xFLAG peptide (200 μg/ml; Sigma-Aldrich; MDYKDHDGDYKDHDID YKDDDDK) at 4°C for 30 min. Elution was performed four times in total, and the combined eluates were diluted with ChIP lysis buffer (to a concentration of 100 μg/ml 3xFLAG peptide), and were subjected to a second immunoprecipitation using an anti-Pk antibody. All steps after the second immunoprecipitation were the same as for standard ChIP analysis.

Northern blot analysis

Northern blot analyses were conducted as described previously (2). For the detection of the *TEF2* and *ADE2-C* reporter genes, DNA fragments were amplified by PCR using the primer pairs TK6965–TK6966 (*TEF2*) and

TK10425–TK10426 (*ADE2-C*) and were then ^{32}P-labelled using random priming.

5′ RLM-RACE

5′ RLM-RACE (RNA Ligase Mediated Rapid Amplification of cDNA Ends) analysis was conducted as previously described (41), using the FirstChoiceTM RLM-RACE Kit (Ambion) with total RNA from H2450 (WT) and YTK8276 (*Δhmo1*) strains. The experiment was conducted according to the instruction manual of the manufacturer (http://www.ambion.com/jp/techlib/prot/fm_1700.pdf). The nested PCR was conducted using universal primers, which bind the RNA adaptor region, and gene-specific primers TK10942 (outer)/TK11567 (inner) for *RPS5* or TK11350 (outer)/TK9589 (inner) for *RPL27B*.

RESULTS

Δhmo1 complements growth defects and reverses a TSS shift due to an *rpb1* mutation in a subset of RPGs

In a previous study, we showed that *Δhmo1* caused an upstream TSS shift in Hmo1-enriched RPGs and suppressed the temperature sensitive growth of some *sua7* mutants (e.g. *sua7-R78C, -E62K*), which caused a downstream TSS shift in many class II genes (23). To determine whether the suppressive effect of *Δhmo1* is specific to *sua7* mutants, we tested for a genetic interaction between *HMO1* and *RPB1*, which encodes the largest Pol II subunit. The mutations, *rpb1-N445S* (42) and *rpb1-R344A* (43), are in or near to the active centre of Pol II, and cause a downstream TSS shift. As previously reported (42,43), both *rpb1* mutants showed significant growth defects at all temperatures tested, and no growth at 37°C (Figure 1A). In contrast, *Δhmo1* cells showed less severe growth defects at high temperature than at low temperature. Importantly, *Δhmo1* suppressed the growth defect of the *rpb1* mutant at 37°C (Figure 1A), as observed for the *sua7* mutants (23).

Next, we tested the effect of these *rpb1* mutations on the TSS in the *RPS5* and *ADH1* promoters by primer extension analysis in the same strains. As previously reported, both *rpb1* mutants caused a downstream shift of the TSS in both promoters (Figure 1B and C, lanes 1–3 and 7–9); namely, the ratios of the intensities of the major band and lower bands were altered modestly (*RPS5*; −36 versus −22) or significantly (*ADH1*; −38 versus −27). In contrast, *Δhmo1* caused an upstream shift of the TSS specifically in the *RPS5* promoter (Figure 1B and C), one of the most Hmo1-enriched and transcriptionally Hmo1-dependent RPGs, but not in the *ADH1* promoter, which binds Hmo1 weakly and is transcriptionally independent of Hmo1 (Figures 1B and C, compare lanes 7 and 10). Briefly, compared to WT cells, in *Δhmo1* cells we observed a decrease in the intensity of two minor bands (−26 and −22, Figure 1B, left panel) situated below the most intensely stained band, corresponding to the major TSS (−36; marked with an asterisk) in the *RPS5* promoter. We also noticed an increase in intensity of two bands (−71, −87), and the presence of three new bands (−133, −215, −225) for TSSs above the major TSS (Figures 1B and C, compare lanes 1 and 4). Although the upper bands in lane 10 appear stronger than those in lane 7 (Figure 1B), the ratio to the band at −38 (double dagger) was nearly identical in lanes 10 and 7 (Figure 1C).

Note that the upstream TSS shift in *Δhmo1* cells can be also detected by another method, 5′ RLM-RACE. The 5′ RLM-RACE is a modified 5′ RACE to amplify selectively the 5′-end of full-length mRNA that contains a base corresponding to TSS. The TAP-dependent bands, which were amplified by PCR, reflect the intact 5′-end of mRNAs of *RPS5* (Supplementary Figure S1A, lane 1 and 3). The result shows that TSSs of *RPS5* were shifted upstream in *Δhmo1* cells (Supplementary Figure S1A, compare lane 1 and 3). A similar result was obtained with the same analysis for *RPL27B* (Supplementary Figure S1B, compare lane 1 and 3), which showed a more drastic TSS shift than *RPS5* in *Δhmo1* cells (Supplementary Figure S2A). The results indicate that the upstream TSS shift that was identified by primer extension analysis occurred in *Δhmo1* cells.

Importantly, *Δhmo1* partly reversed the TSS shift in the *RPS5* promoter (Figure 1B and C, compare lanes 1, 4, 5 and 6) but not in the *ADH1* promoter (Figure 1B and C, compare lanes 7, 10, 11 and 12) in both *rpb1* mutants. This effect was stronger in the *Δhmo1 rpb1-R344A* mutant (Figure 1B and C, compare lanes 1 and 5, 6), consistent with the observation that *Δhmo1* suppressed the growth defect of *rpb1-R344A* more strongly than for *rpb1-N445S* (Figure 1A). These results suggested that *Δhmo1* suppresses the growth defects of *rpb1* mutants by reversing the TSS shift in certain Hmo1-enriched and transcriptionally Hmo1-dependent genes, such as *RPS5*.

Δhmo1 causes an upstream TSS shift by a different mechanism than *tfg1* or *Δrpb9*

While all mutant genes that are known to cause the upstream TSS shift encode subunits of Pol II or limited components of PIC (30–37), only Hmo1 is not a component of PIC. This suggests that the upstream TSS shift in *Δhmo1* is caused by a different mechanism than in other mutants. Therefore, its mechanism may involve a specialized function(s) of Hmo1 with respect to the regulation of transcriptional initiation at the RPG promoter. To understand the mechanism behind the upstream TSS shift in *Δhmo1* and other mutants, transcriptional phenotypes for *Δhmo1*, Pol II (*Δrpb9*) and TFIIF (*tfg1-E346A*) mutants were compared.

First, we compared the TSS profiles of the *RPS5* and *ADH1* promoters in three single mutants (*Δhmo1*, *tfg1-E346A* and *Δrpb9*) and three double mutants (*Δhmo1 tfg1-E346A*, *Δhmo1 Δrpb9* and *tfg1-E346A Δrpb9*) with those in WT cells. As previously reported (31), the *tfg1-E346A Δrpb9* double mutant exhibited more severe growth defects than either of the single mutants (*tfg1-E346A, Δrpb9*) at 25°C, 30°C and 35°C (Supplementary Figure 3A). Primer extension analyses revealed that the *tfg1-E346A* and *Δrpb9* mutations caused upstream TSS shifts in the *RPS5* and *ADH1* promoters, while the shift

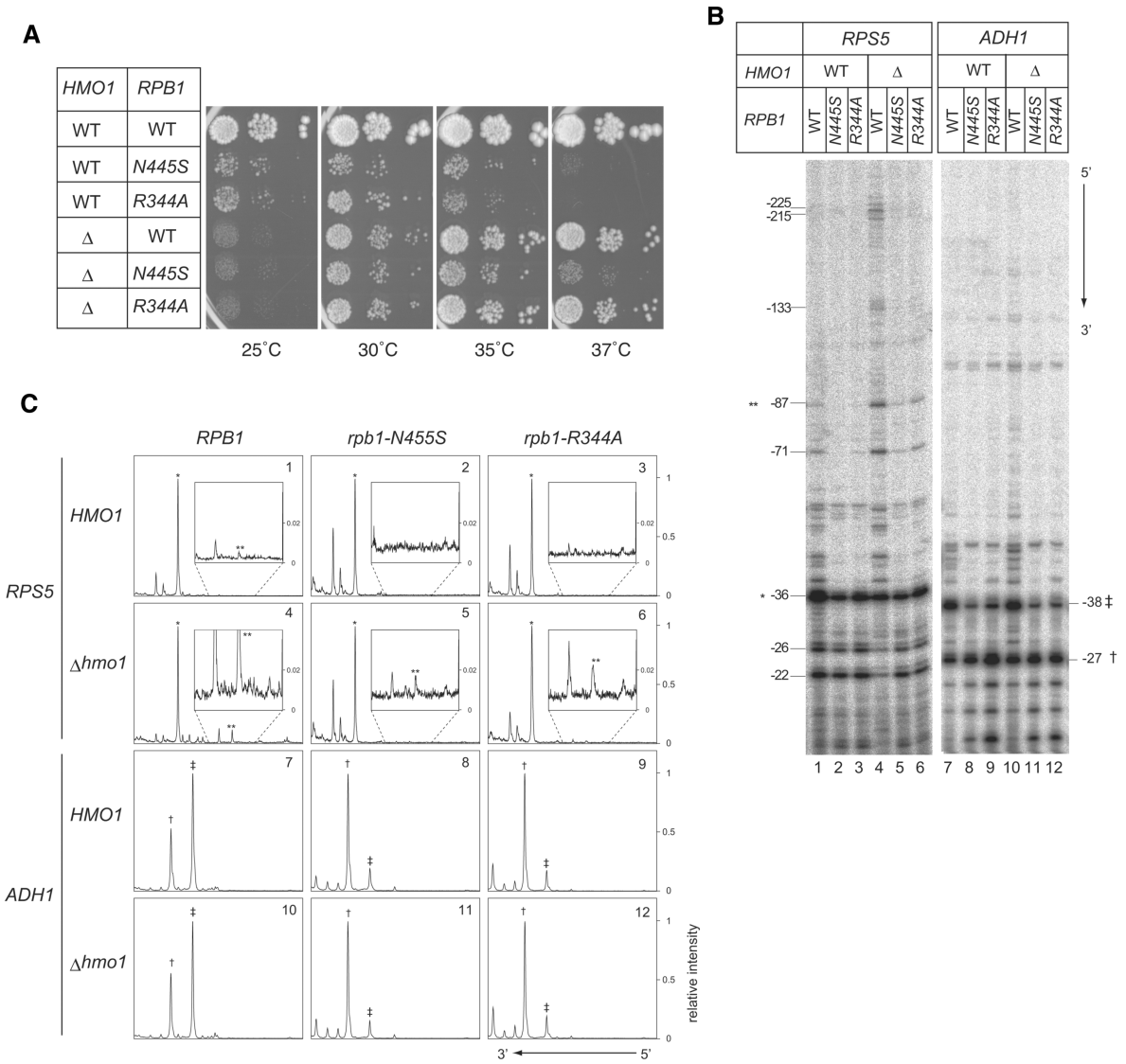

Figure 1. Genetic interaction between *HMO1* and *RPB1*. (**A**) Effect of *Δhmo1* and/or *rpb1* mutations on growth. *Δrpb1* and *Δrpb1 Δhmo1* cells carrying a plasmid encoding the *RPB1* (WT) or *rpb1* mutant (N445S, R344A) were spotted onto YPD (yeast extract, peptone, dextrose) plates at three dilutions and grown for 3 days (30°C, 35°C and 37°C) or 4 days (25°C). (**B**) Effect of *Δhmo1* and/or *rpb1* mutations on the TSS in *RPS5* and *ADH1* promoters. The strains described in (A) were grown at 25°C. Total RNA (15 μg) was prepared and analysed by primer extension. The positions of several TSSs are indicated on the left (*RPS5*) or right (*ADH1*). TSSs are numbered relative to the A (+1) of the start codon, ATG (−22, −26, −36, −71, −87, −133, −215 and −225 for the *RPS5* promoter and −27 and −38 for the *ADH1* promoter). TSSs at −36 and −87 in the *RPS5* promoter and −27 and –38 in the *ADH1* promoter are marked with asterisks (* and **) and daggers († and ‡), respectively. (**C**) Results shown in (B) were quantified by densitometry. The number in the upper right corner of each panel corresponds to the lane number in (B). Values were normalized to the strongest peak in each panel (i.e. strongest peak set to a value of 1). The horizontal axis represents the position of each band within the region shown in (B). Note that the regions shown in (B) and (C) are identical. Asterisks (* and **) and daggers († and ‡) correspond to the bands at −36 and −87 (*RPS5*), and those at −27 and −38 (*ADH1*), respectively, as shown in (B). Part of the scanned region was enlarged and is shown in the inset to highlight the differences.

in each promoter was enhanced in the double mutant (Supplementary Figure S3B and C). Consistent with a previous study (30), although the degree of TSS shift was slightly different between *tfg1-E346A* and *Δrpb9*, the positions of the upstream TSS in both promoters were nearly the same in both mutants (Supplementary Figure S3B and C, compare lanes 2, 6 and 3, 7, respectively), suggesting that the mechanism for the TSS shift may be similar in these mutants.

In contrast, the feature of TSS shift was quite different in *Δhmo1* and *tfg1-E346A* mutants (Figure 2). Primarily, *tfg1-E346A* caused an upstream TSS shift in all promoters tested (*RPS5, ADH1*, *SPT15, HTB1, GAL1, GAL10, HIS3, HIS4, SNR7, SNR14, SNR19* and *SNR20*) [in this study, and (30)], while *Δhmo1* shifted the TSS specifically in the Hmo1-enriched RPG promoters, e.g., *RPS5, RPL32* (23), and *RPL27B* (Supplementary Figure S2A). Furthermore, it is

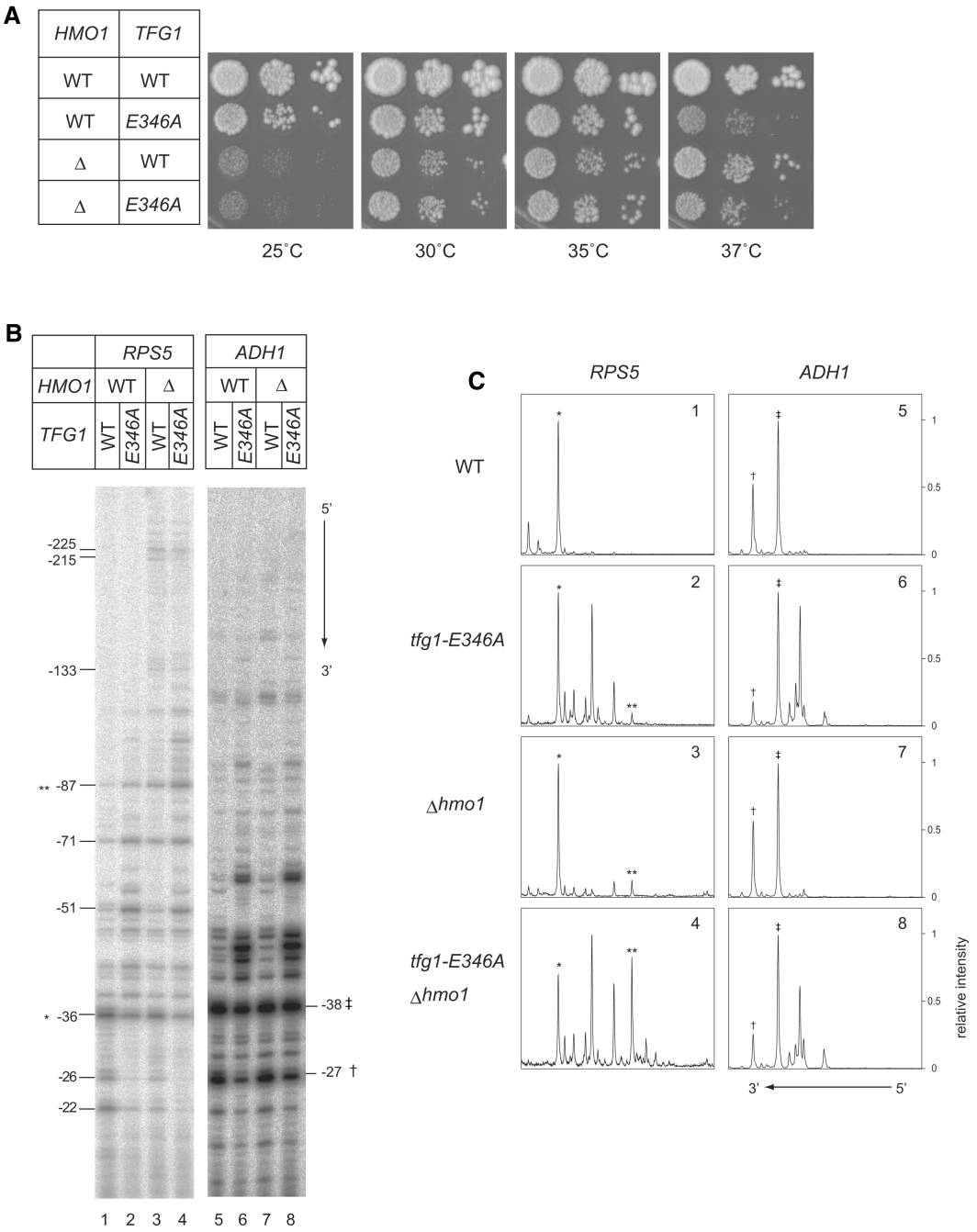

Figure 2. Genetic interaction between *HMO1* and *TFG1*. (**A**) Effect of *Δhmo1* and/or *tfg1-E346A* on growth. Growth of *Δtfg1* and *Δtfg1 Δhmo1* cells carrying the plasmid encoding *TFG1* (WT) or *tfg1-E346A* was analysed as described in Figure 1A. (**B**) Effect of the *Δhmo1* and/or *tfg1-E346A* mutation on the TSS in *RPS5* and *ADH1* promoters. Yeast strains were as indicated in (A). Cells were grown at 25°C, and total RNA (15 μg) was prepared and analysed by primer extension as described in Figure 1B. (**C**) Results shown in (B) were quantified and the data are summarized as described in Figure 1C.

noteworthy that transcription from −51A in the *RPS5* promoter was markedly enhanced by *tfg1-E346A*, but not by *Δhmo1* (Figure 2B, lanes 1–4). Conversely, TSSs around −220 (−215 and −225) were induced uniquely by *Δhmo1* (Figure 2B, lanes 1–4). Similar but weaker effects were observed in *Δhmo1, Δrpb9* and *Δhmo1 Δrpb9* cells (Figure 3, lanes 1–4). These results suggested that the mechanism(s) underlying the TSS shift in the *Δhmo1* cells might be different from that in the TFIIF/Pol II mutants. However, direct evidence will be required to confirm this possibility.

Although the *Δhmo1 tfg1-E346A* double mutant had more severe synthetic effects on the TSS compared to either of the single mutants, we found no obvious synthetic growth defect for this double mutant when compared to the single mutants. A similar result was obtained for the *Δhmo1 Δrpb9* double mutant (data not shown). Therefore, it seems unlikely that the upstream TSS shift itself is the

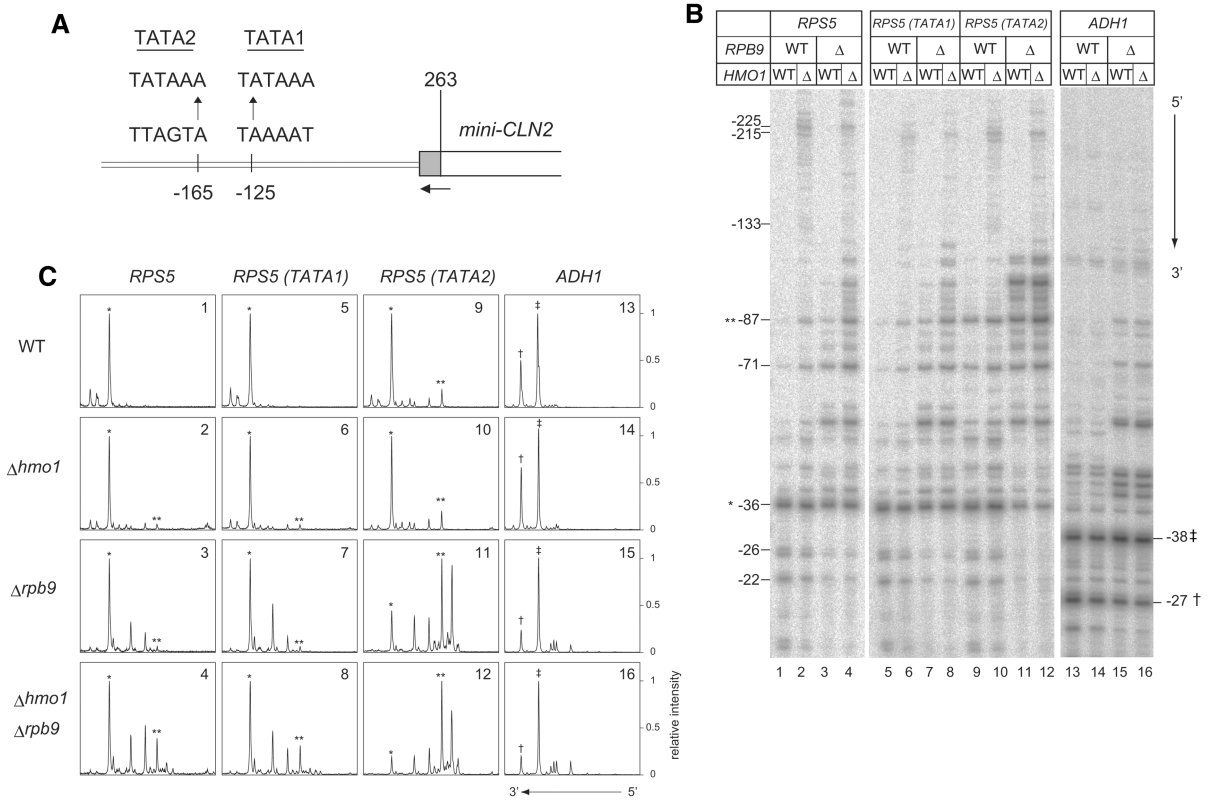

Figure 3. Effects of artificial recruitment of TBP/TFIID to upstream regions of the core promoter on upstream TSS shift in *Δrpb9* and/or *Δhmo1* cells. (**A**) Schematic diagram depicting ectopic TATA elements inserted into the *RPS5* promoter. *RPS5* promoters with or without an ectopic TATA element at −125 (TATA1) or −165 (TATA2) were fused to a *mini-CLN2* reporter gene and inserted into a plasmid. A 16-bp DNA fragment (5′-CTTGCTGTCAGCGATC-3′) was inserted between the *RPS5* promoter and *mini-CLN2* (indicated with a grey square). This sequence was used to discriminate between mRNA produced from the endogenous *RPS5*/*CLN2* or from *mini-CLN2*. The primer, TK9911, used for the primer extension is indicated with an arrow. (**B**) Effect of *Δhmo1* and/or *Δrpb9* on the TSS in *RPS5* promoters, with or without an ectopic TATA element, was analysed by primer extension. The plasmid containing one of the three *RPS5* promoters (original, TATA1 or TATA2) was transformed into WT, *Δhmo1, Δrpb9* and *Δhmo1 Δrpb9* cells. Transformants were selected on YPD medium containing aureobacidin A (0.2 μg/ml). Total RNA (15 μg) from these strains, which were grown in the same medium at 25°C, was analysed by primer extension as described in Figure 1B. (**C**) Results shown in (B) were quantified and summarized as described in Figure 1C.

major determinant for the growth defects in these mutants (single and double).

Because *Δhmo1* decreased the binding of Fhl1 to the RPG promoter (2,22), it is possible that the upstream TSS shift in *Δhmo1* cells is the result of the dissociation of Fhl1 from the *RPS5* promoter. This was tested by analysing the TSS of *RPS5* in *Δfhl1* cells by primer extension analysis. Although *Δfhl1* shifts the TSS of *RPS5* modestly as compared with WT, the extent of the TSS shift was less severe in *Δfhl1* cells than in *Δhmo1* cells (Supplementary Figure S2B; TSSs upstream of −87 were not observed in *Δfhl1* cells). Given that *Δfhl1* decreases the Hmo1 binding to a subset of RPG promoters (22), the TSS shift in *Δfhl1* cells may be related to a decrease in Hmo1 binding rather than the direct effect of the loss of Fhl1 function. However, *Δhmo1* caused a less pronounced upstream TSS shift in an Hmo1-enriched RPG, *RPS18A*, whose binding to Fhl1 was not affected in *Δhmo1* cells (2), than in the *RPS5* promoter (Supplementary Figure S2C). Therefore, it cannot be excluded that Fhl1 has also a direct role in the selection of the correct TSS.

Besides RPG promoters, Hmo1 also binds abundantly to a subset of non-RPG promoters (2,22). Therefore, we tested whether *Δhmo1* caused upstream TSS shifts in these promoters. Remarkably, the TSS of *FET3*, a non-RPG with strong Hmo1 binding activity, was not affected in *Δhmo1* cells (Supplementary Figure S2D), suggesting that the function of Hmo1 at non-RPG promoters may be different from that at RPG promoters.

Upstream TSS shift is caused by a pre-PIC assembly defect in *Δhmo1* cells and by a post-PIC assembly defect in *Δrpb9* cells

In *S. cerevisiae*, a 'scanning model' has been proposed to explain TSS selection by Pol II (44–46). In this model, following PIC assembly at the core promoter, Pol II starts scanning downstream and initiates transcription when it encounters an appropriate TSS. According to this model, two different mechanisms for an upstream TSS shift seem possible. The first mechanism involves normal PIC assembly, followed by a defect in the post-PIC assembly function of Pol II, while the second mechanism proposes an upstream shift of the PIC

assembly site, reflecting a pre-PIC assembly defect but a normal post-PIC assembly function of Pol II.

The *tfg1*, *tfg2*, *rpb2* and *Δrpb9* mutants are thought to cause upstream TSS shifts via the post-PIC assembly defect, while *Δhmo1* causes the TSS shift by a different mechanism, presumably the pre-PIC assembly defect. If a TSS shift is due to relocation of the PIC assembly site upstream in *Δhmo1* cells, we predicted that insertion of a TATA element to induce upstream PIC assembly artificially would not alter the TSS significantly in *Δhmo1* cells, but would cause a significant TSS shift in WT cells. As a result, the TSS pattern in WT and *Δhmo1* cells would be similar. In contrast, if the TSS shift is caused by a post-PIC assembly defect, such as a change in Pol II activity, we predicted that insertion of an upstream TATA element would generate novel TSS patterns in both WT and *Δhmo1* cells, and that these patterns would be different. To test this hypothesis, an ectopic TATA element was engineered at two upstream positions, −125 (TATA1) or −165 (TATA2), in the *RPS5* promoter (Figure 3A). The original or modified *RPS5* promoters were fused to a mini-*CLN2* reporter gene, a non-functional *CLN2* lacking part of the ORF (47), and inserted into a low-copy number plasmid. Importantly, the *RPS5* promoter on the plasmid had almost identical properties to the chromosomal *RPS5* promoter, including abundant Hmo1 binding, Hmo1-dependent Fhl1 binding, and TSS profiles in WT, *Δhmo1* and/or *Δrpb9* cells (Supplementary Figure S4A and B, and data not shown). Primer extension analyses were conducted using WT, *Δhmo1*, *Δrpb9* and *Δhmo1 Δrpb9* cells, each containing a mini-*CLN2* reporter plasmid carrying the *RPS5*, *RPS5-TATA1* or *RPS5-TATA2* promoters (Figure 3B and C). In all strains tested, *RPS5-TATA1* had no significant effect on the TSS, possibly because the endogenous PIC assembly site is close to this site (Figure 3B and C, compare lanes 1–4 with 5–8). On the contrary, *RPS5-TATA2* caused a more modest upstream TSS shift in *Δhmo1* cells than in WT cells (Figure 3B and C, compare lanes 1, 2 and 9, 10, respectively). As the result, the TSS patterns became similar in WT and *Δhmo1* cells, at least in the region downstream of this insertion (Figure 3B, compare lanes 9 and 10). In contrast, *RPS5-TATA2* drastically altered the TSS pattern in *Δrpb9* and *Δrpb9 Δhmo1* strains (Figure 3B and C, compare lanes 3, 4 and 11, 12). As the result, the TSS patterns of the *RPS5-TATA2* promoter in *Δrpb9* and *Δrpb9 Δhmo1* became significantly different from those in WT and *Δhmo1* (Figure 3B and C, compare lanes 9, 10 and 11, 12). These results suggested that *Δhmo1* shifts the TSS by relocating the PIC assembly site upstream, while *Δrpb9* shifts the TSS by causing a defect(s) in Pol II activity at a post-PIC assembly step.

An intervening region between the UAS and the core promoter is required for Hmo1 binding and the upstream TSS shift caused by *Δhmo1* in Hmo1-enriched RPG promoters

Δhmo1 caused an upstream TSS shift in the Hmo1-enriched *RPS5* promoter, but not in the Hmo1-limited *RPL10* promoter (23). Therefore, to identify the *RPS5* promoter region responsible for this shift in *Δhmo1* cells, we constructed a series of chimeric promoters in which the UAS, Core or IVR of *RPS5* and *RPL10* were mutually exchanged (Figure 4A). These modified promoters were integrated into the *ADE2* chromosomal locus in WT or *Δhmo1* cells. Primer extension analysis for these strains clearly revealed that the IVR of *RPS5* was required for an upstream TSS shift in *Δhmo1* cells (Figure 4B) while the UAS and Core of *RPS5* can be exchanged for those of *RPL10* without blocking the TSS shift.

RPL27B showed almost the same properties as *RPS5* with respect to Hmo1 binding, Hmo1-dependent transcription and Fhl1 binding. As expected, *Δhmo1* also induced an upstream TSS shift in an additional chimeric promoter, constructed from the IVR of *RPL27B* and the UAS and Core of *RPL10* (Figure 4A and B, lanes 17 and 18), implying that the IVR of Hmo1-enriched RPGs is a critical determinant for the TSS shift in *Δhmo1* cells.

These results suggested that the IVRs in the *RPS5* and *RPL27B* promoters are also required for abundant Hmo1 binding to these promoters. In fact, ChIP analyses revealed that Hmo1 binds abundantly to promoters containing the *RPS5*- or *RPL27B*-IVR, but not to those containing the *RPL10*-IVR (Figure 4C, panels 1 and 2). The roles of the IVR, UAS and Core in supporting abundant Hmo1 binding were examined by ChIP analyses of *RPS5* promoters lacking each of these segments. The results clearly revealed that the IVR is essential, but the UAS and Core are dispensable, for Hmo1 binding (Figure 4C, panels 3 and 4). Previously, Hall *et al.* (22) reported that Hmo1 binding to the *RPS11B* promoter at the *HIS3* chromosomal locus was dependent on Rap1 binding sequences. Therefore, we used ChIP analysis to test whether our deleted UAS (*Δ*UAS) construct contained a cryptic Rap1 binding site. The result confirmed that Rap1 was absent from this construct (Supplementary Figure S5A and B). Furthermore, the *Δ*UAS construct showed much weaker transcription than WT. These results excluded the possibility that a cryptic Rap1 (or Abf1) binding site would decrease Rap1-dependency of Hmo1 binding in our *Δ*UAS construct. It is possible that Rap1-dependency of Hmo1 binding differs at each genomic locus.

Further mapping analysis, using a series of promoter constructs, in which 40-bp segments in the *RPS5* promoter were deleted systematically, found no segments that were indispensable for Hmo1 binding (data not shown). However, ChIP analysis using promoter constructs, in which the *RPS5*-IVR between the UAS and Core of *RPL10* was deleted serially from upstream or downstream, revealed at least two non-overlapping sequences that supported abundant Hmo1 binding in the *RPS5*-IVR (−439 to −260 bp and −259 to −127 bp; Supplementary Figure S6A and B). In addition, the −319 to −199 bp region (120 bp), which overlaps these two regions, also supported full Hmo1 binding (data not shown). Thus, abundant Hmo1 binding to the *RPS5*-IVR occurs by the independent or cooperative functioning of multiple specific Hmo1 binding sites.

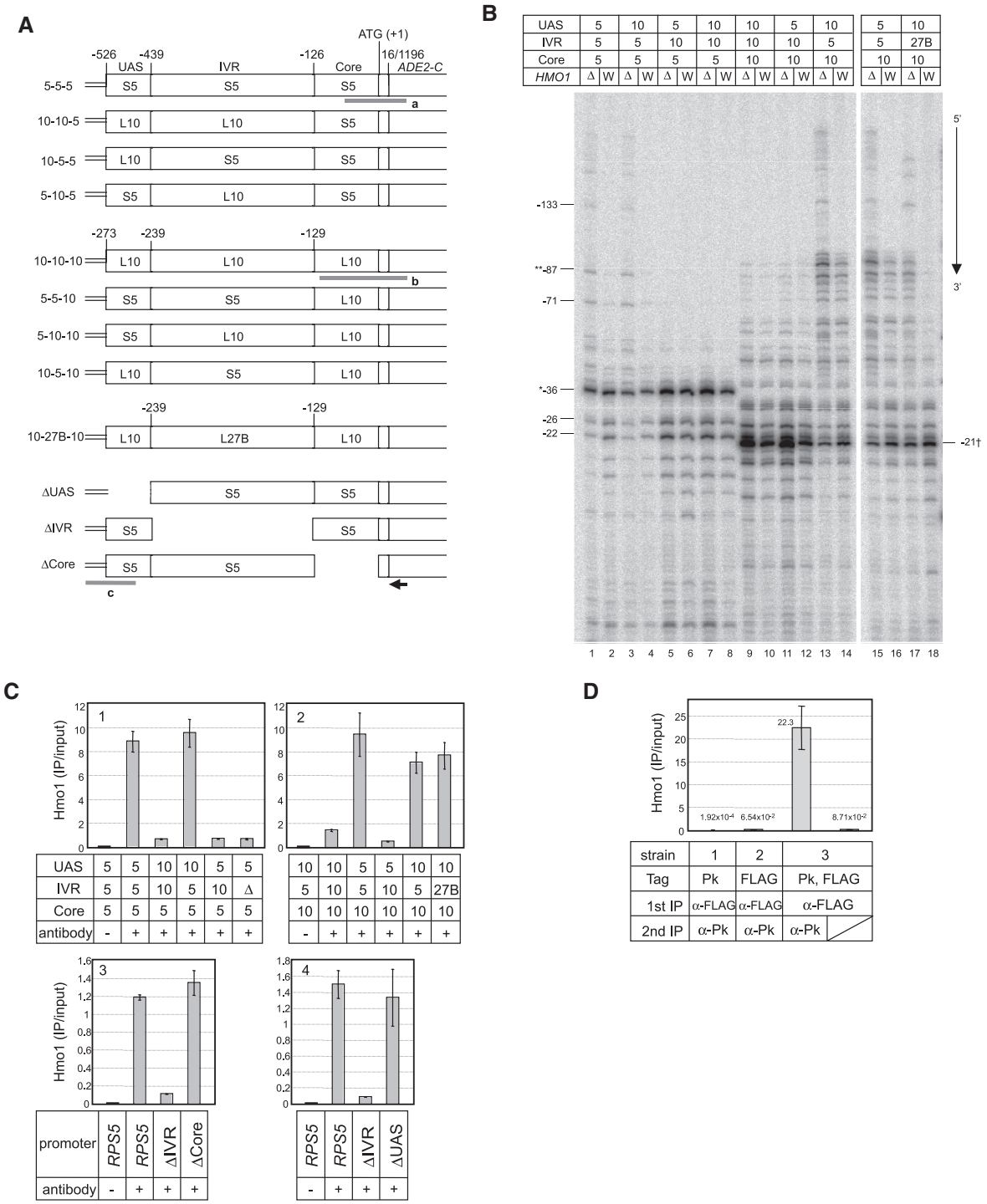

Figure 4. Mapping of the promoter region required for Hmo1 binding and upstream TSS shift in *Δhmo1* cells. (**A**) Schematic diagram depicting chimeric *RPS5*/*RPL10* promoters, *RPS5* promoters lacking one of three segments (UAS, IVR or Core), or a promoter containing the *RPL27B*-IVR. The designation indicated at the left is an abbreviation of each promoter construct. For instance, '5-5-5' at the top denotes a construct that contains *RPS5*-UAS, *RPS5*-IVR, and *RPS5*-Core (+16 bp of 5′ region of *RPS5* ORF). All modified promoters were fused to *His3MX6* by PCR and then integrated into the *ADE2* locus with an accompanying deletion of an ~1.2-kb DNA region encoding the N-terminal portion of Ade2. The regions amplified by PCR in the ChIP assays are underlined and labelled 'a', 'b' or 'c'. The primer TK10595, used for primer extension, is indicated with an arrow. (**B**) The promoter region required for the upstream TSS shift in *Δhmo1* was analysed by primer extension, as described in Figure 1B. The TSSs of the chimeric promoters, described in (A), were examined in *Δhmo1* (odd-numbered lanes; *Δ*) or WT cells (even-numbered lanes; W). TSSs at −36 and −87 in the *RPS5*-Core and −21 in the *RPL10*-Core are marked with asterisks (* and **) and dagger (†), respectively. (**C**) Hmo1 binding to the test promoters described in (A) was analysed *in vivo* by ChIP assays. The strains carrying modified promoters and expressing Hmo1-FLAG were grown in YPD medium to mid-log phase at 25°C. Cross-linked chromatin was prepared and immunoprecipitated with an anti-FLAG antibody (0.1 μg) and Dynabeads Protein G. Immunoprecipitation was also conducted using an anti-Myc antibody (1 μg) as a negative control (indicated as '−'). Panels 1 and 4 summarize the results for the promoters that contain the *RPS5*-Core (region 'a' is amplified). Panel 2 summarizes the results for

(continued)

Alternatively, the length of the IVR might be more critical for Hmo1 binding than a specific DNA sequence because a correlation was observed between the length of the IVR and Hmo1-binding in our deletion analysis of *RPS5*-IVR (Supplementary Figure S6B) or in endogenous RPG promoters (22) (our unpublished data). To address this possibility, we constructed several promoter constructs that contained different DNA fragments, e.g. a non-promoter sequence from chromosome V (Chr. V) of *S. cerevisiae* or pBR322 plasmid, or triplicate *RPL10*-IVR, between the UAS and Core of *RPL10* (Supplementary Figure S6C). Using these modified promoter constructs, the ChIP analysis revealed that while *RPS5*-IVR (−439 to −260; 180 bp) bound similar levels of Hmo1 as full-length *RPS5*-IVR, two unrelated sequences of similar lengths showed modest (pBR322) or no (Chr. V) Hmo1 binding (Supplementary Figure S6D). Similarly, triplicate *RPL10*-IVR, which is longer than *RPS5*-IVR, could not bind Hmo1 (Supplementary Figure S6D). These results suggest that a specific sequence of DNA is more critical than the length of the DNA for Hmo1 binding.

The finding that multiple Hmo1 binding sites exist in *RPS5*-IVR raised the additional question of whether more than two Hmo1 molecules can bind to an *RPS5* promoter simultaneously. To address this question, we conducted sequential ChIP analysis using strains expressing a Hmo1-FLAG tag and/or Hmo1-Pk tag. After sequential immunoprecipitation using anti-FLAG antibody (first) and anti-Pk antibody (second), DNA containing the *RPS5*-IVR was recovered efficiently (Figure 4D). This result clearly indicated that more than two Hmo1 molecules bind to an *RPS5*-IVR *in vivo,* although it is unclear whether they bind to different binding sites.

The PIC assembles at a site between the +1 nucleosome and a nucleosome-free IVR bound by Hmo1

To confirm the binding of Hmo1 to the *RPS5*-IVR, we conducted high-resolution ChIP analyses for Hmo1-enriched RPG promoters (*RPS5* and *RPL27B*). The results clearly showed that Hmo1 binds to the IVRs of these promoters (Figure 5A, panels a and c). In addition, similar results were obtained for Hmo1-enriched, non-RPG promoters such as *HMO1* (Figure 5A, panel g), suggesting that Hmo1 tends to bind the IVR of its target promoters. Interestingly, Hmo1 even binds to the IVR of the Hmo1-limited *RPL10* promoter (Figure 5A, panel e).

Next, we compared the Hmo1 binding site with those of other factors like Rap1, TFIIB (Sua7; a PIC component) and histone H3 (nucleosome) on the same promoters. ChIP analyses showed that Rap1 binds to the UAS of the *RPS5*, *RPL27B* and *RPL10* promoters but not to any region of the *HMO1* promoter (data not shown). This is consistent with our notion that Rap1-dependentcy of Hmo1 binding may differ depending on the locus. Remarkably, ChIP analyses also showed that the *RPS5*-IVR is nucleosome-depleted (Figure 5A, panel a) and that the PIC assembles at a site between the binding peaks of Hmo1 and a nucleosome (3′-side) on the *RPS5* promoter (Figure 5A, panel b). Similar binding properties for Hmo1, TFIIB and histone H3 were observed for the other two Hmo1-enriched promoters (*RPL27B* and *HMO1*, Figure 5A, panels c,d and g,h, respectively).

Recent ChIP-seq studies revealed that many class II gene promoters have two well-positioned nucleosomes (−1 and +1) (48). The −1 nucleosome, located 150–300 bp upstream of the TSS, regulates the access of transcription factors to this region, while the upstream boundary of the +1 nucleosome lies 10–15 bp upstream of the TSS (49,50). As a result, a relatively wide NFR (∼140 bp) is formed between these two nucleosomes. Intriguingly, RPG promoters have a significantly broader NFR than other promoters, possibly due to the lack of the −1 nucleosome (48). Our results showed that, in Hmo1-enriched promoters, Hmo1 apparently binds to the position occupied by the −1 nucleosome in other promoters.

The spatial arrangement of the PIC, +1 nucleosome and Hmo1 within Hmo1-enriched promoters suggests that Hmo1 and the +1 nucleosome direct assembly of the PIC to a specific site. In this regard, Hmo1 is a novel transcription factor involved in determining the 5′-border of a region available for PIC assembly within the core promoter. In contrast to Hmo1-enriched promoters (*RPS5*, *RPL27B* and *HMO1*), the binding peaks of Hmo1 and PIC overlapped in the *RPL10* promoter (Figure 5A, panels e and f). Although there was no evidence to exclude the possibility that Hmo1 and the PIC bind together at the same position in the *RPL10* promoter, we assume this is due to limitations of the ChIP resolution in the relatively narrow *RPL10*-IVR. As an alternative possibility, Hmo1 and PIC could bind to the same position, but in different cell populations.

The binding profiles of Hmo1 and nucleosomes raised the possibility that Hmo1 may inhibit nucleosome formation on the IVR. To test this possibility, we used ChIP analysis to compare histone H3 binding profiles in WT and *Δhmo1* cells. The results showed that the *RPS5* promoter has a similar NFR in both cell types despite the slight increase in histone H3 binding in *Δhmo1* cells (Figure 5B), suggesting that Hmo1 does not play a critical role in the formation and/or maintenance of NFRs.

Δhmo1 shifts the PIC assembly site upstream in the *RPS5* promoter

The results described above suggested that Hmo1 and the +1 nucleosome determine the 5′- and 3′-border,

Figure 4. Continued
the promoters that contain the *RPL10*-Core (region 'b' is amplified). Panel 3 summarizes the results for the promoters that contain the *RPS5*-UAS (region 'c' is amplified). (**D**) Simultaneous binding of more than two Hmo1 molecules to an *RPS5*-IVR was tested by sequential ChIP analysis. The strains expressing Hmo1-FLAG and/or Hmo1-Pk were grown in YPD medium to mid-log phase at 25°C, cross-linked chromatin was prepared, and the samples were subjected to sequential immunoprecipitation using an anti-FLAG antibody (first) and an anti-Pk antibody (second). PCR was conducted for the *RPS5*-IVR (region '5' in Figure 5A). The result is reliable because amplification occurred only when immunoprecipitation was conducted using both antibodies against chromatin from yeast cells expressing both of the different Hmo1 species (strain 3).

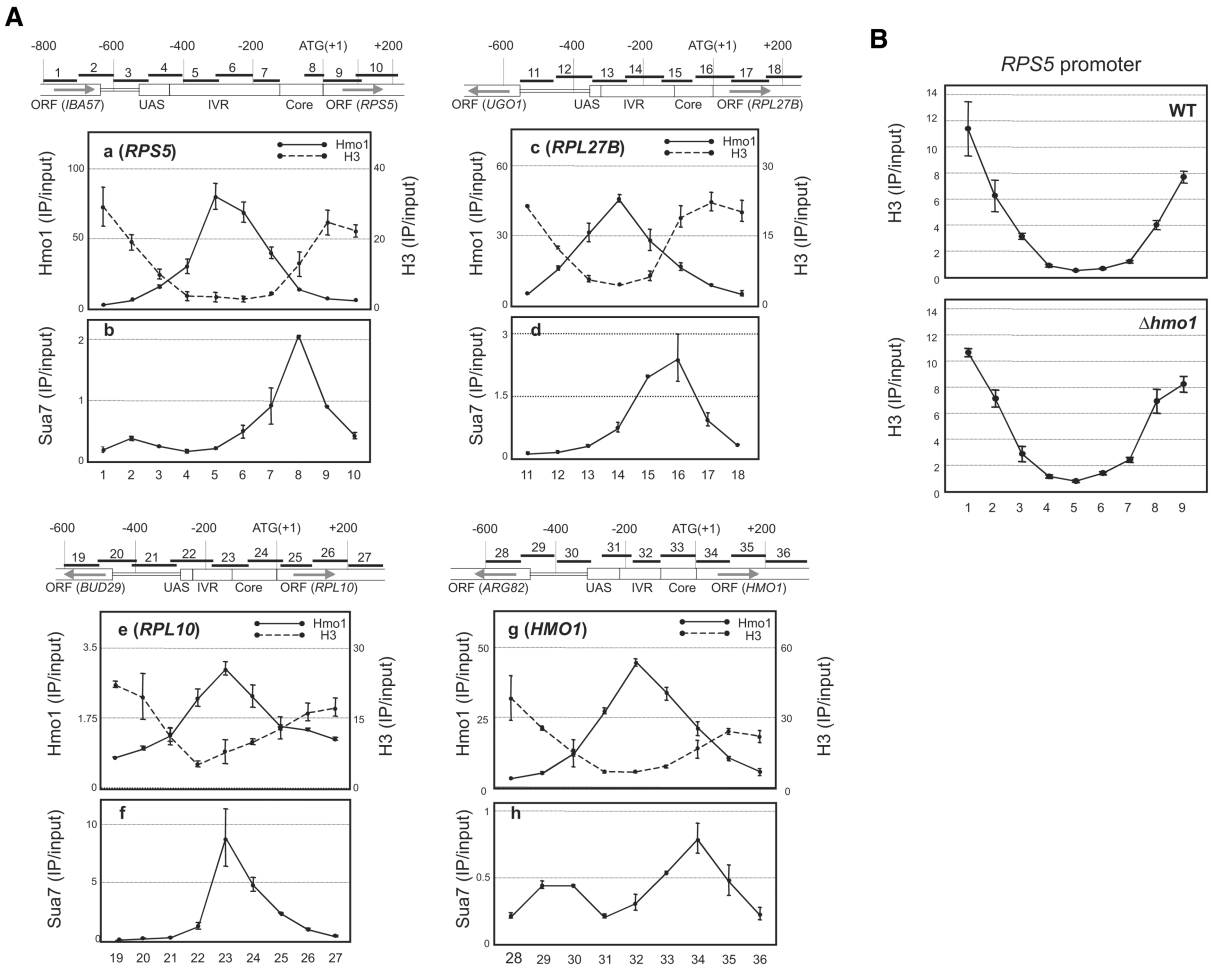

Figure 5. Identification of exact binding sites for Hmo1, nucleosome and PIC in Hmo1-enriched and Hmo1-limited promoters. (**A**) Exact binding sites for Hmo1, nucleosome and PIC were identified in several promoters by high-resolution ChIP analyses. The schematic diagrams depicting the endogenous promoter regions tested are indicated above the panels, which summarize the results for each promoter (*RPS5*, *RPL27B*, *RPL10* and *HMO1*). These promoters were divided into UAS, IVR and Core based on information for certain promoter elements (see Supplementary Data). The grey arrows represent the direction of the ORF. The black bars closely aligned to the entire promoter (and part of the ORF) of each gene represent the regions amplified by PCR in ChIP assays. ChIP analyses were conducted as described in Figure 4C, except that chromosomal DNA was fragmented to an average size of 100–200 bp. The ChIP results for Hmo1 (+Pk tag) and histone H3 are indicated in the upper panels (a, c, e, g) with a solid line or broken line, respectively, while results for TFIIB (Sua7-Pk) are indicated in the lower panels (b, d, f, h). The numbers indicated under the panels ('1'–'36') correspond to the regions depicted in the schematic diagram. (**B**) The binding profiles of histone H3 on the *RPS5* promoter were analysed in WT and *Δhmo1* cells by ChIP analysis as described in (A).

respectively, of the PIC assembly zone. If this is so, *Δhmo1* should disrupt the 5′-border of this zone, allowing ectopic PIC assembly on the IVR. An effect that induces ectopic PIC assembly could account for the upstream TSS shift in *Δhmo1* cells. To test this possibility directly, ChIP analysis was conducted to determine the binding positions of several PIC components including TFIIB (Sua7), TFIIF (Tfg1), TFIIE (Tfa2) and TFIIH (Tfb3) on the *RPS5* promoter in WT and *Δhmo1* cells. The binding positions of these factors were shifted upstream in *Δhmo1* cells (i.e. from position 8 to 7; Figure 6B, compare panels a, c, e, g with panels b, d, f, h, respectively). Our recent mapping analysis for core promoter elements in the *RPS5* promoter revealed that the region corresponding to position 7 cannot bind PIC in the native context in the WT cells, although it can induce PIC assembly when artificially inserted into a different context (51). Therefore, the upstream shift of the PIC assembly site observed in *Δhmo1* cells reflects the ectopic PIC assembly in this region (approximately position 7), where PIC intrinsically does not assemble in WT cells. In contrast, a similar upstream shift in the binding position of the PIC component (Sua7) was not observed in *tfg1-E346A* and *Δrpb9* cells (Figure 6C), indicating that the upstream TSS shift in these mutants was caused by a post-PIC assembly defect. Therefore, we concluded that Hmo1 cooperates with the +1 nucleosome to direct PIC assembly to a site between the IVR and the +1 nucleosome by determining the 5′- and 3′-boundaries of a zone available for PIC assembly.

DISCUSSION

In this study, we aimed to find a function for Hmo1 in the regulation of transcriptional initiation of Hmo1-enriched

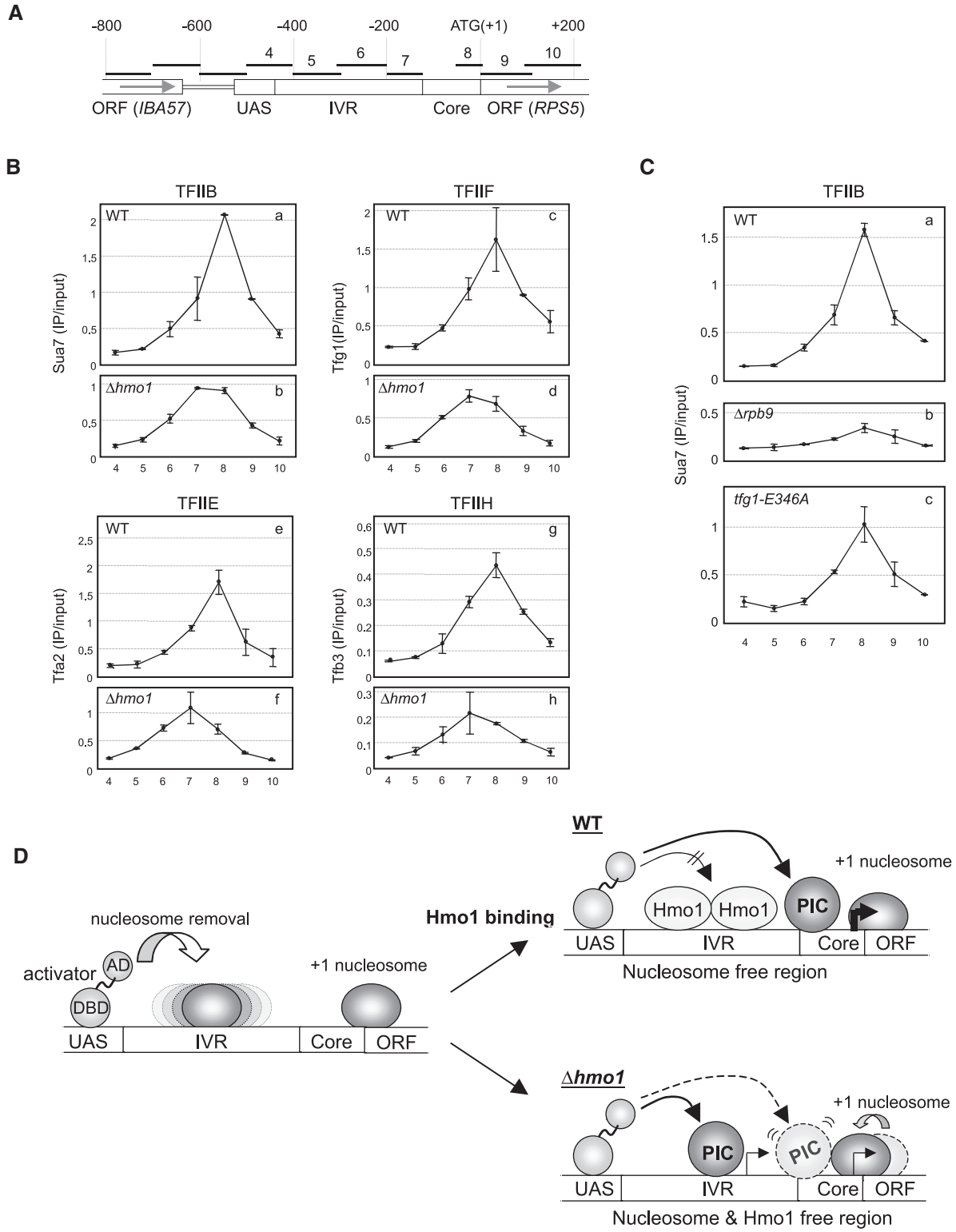

Figure 6. *Δhmo1* shifts the PIC assembly site upstream in the *RPS5* promoter. (**A**) Schematic diagram depicting the endogenous *RPS5* promoter. (**B**) Analysis of the effect of *Δhmo1* on the position of PIC assembly on the *RPS5* promoter. The exact positions of several PIC components including TFIIB (Sua7-Pk), TFIIF (Tfg1-Pk), TFIIE (Tfa2-Pk) and TFIIH (Tfb3-Pk) on the *RPS5* promoter were determined in WT and *Δhmo1* cells by ChIP analysis as described in Figure 5A. The upper and lower panels for each component indicate the results in WT and *Δhmo1* cells, respectively. The numbers under each panel ('4'–'10') represent the position of regions amplified in the *RPS5* promoter as depicted in Figure 5A. (**C**) Analysis of the effect of *Δrpb9* or *tfg1-E346A* on the position of PIC assembly on the *RPS5* promoter. The TFIIB binding site on the *RPS5* promoter was determined in WT, *Δrpb9* and *tfg1-E346A* cells by ChIP analysis as described in (A), except that immunoprecipitation was conducted by using an anti-Sua7 polyclonal antibody. (**D**) A model for the proposed role of Hmo1 in Hmo1-enriched RPG promoters (DBD, DNA binding domain; AD: Activation domain). See text for description of the model.

RPGs by determining how *Δhmo1* induces a TSS shift in these genes. The results showed that: (i) the upstream TSS shift in *Δhmo1* cells was due to a pre-PIC assembly defect, while the shifts in *Δrpb9* and *tfg1-E346A* cells were caused by a post-PIC assembly defect; (ii) Hmo1 binds over a broad region corresponding to the *RPS5*-IVR, which is nucleosome-depleted; (iii) multiple Hmo1 molecules bind to the *RPS5*-IVR; (iv) PIC assembles at a site flanked by Hmo1 and the +1 nucleosome; (v) Hmo1 does not play a critical role in the formation and/or maintenance of NFRs, at least in the *RPS5* promoter; and (vi) *Δhmo1* causes an upstream shift of the PIC assembly site.

Based on these findings, we proposed a model for a novel function of Hmo1 on its target promoters (Figure 6D). Initially, certain activators on the UAS (e.g. Rap1), remove the nucleosomes around the IVR. In WT cells, Hmo1 then binds to nucleosome-free IVRs to inhibit ectopic PIC assembly in this region, thereby directing PIC assembly to a biologically relevant site in the core promoter (Figure 6D, WT). In contrast, in *Δhmo1* cells, activator(s) facilitate PIC assembly at more proximal site(s) within the IVR, which are devoid of Hmo1 and nucleosomes, leading to an upstream TSS shift (Figure 6D, *Δhmo1*).

While *Δhmo1* does not have a severe effect on NFR in the *RPS5* promoter, it causes a slight increase in histone H3 binding to the core promoter region of *RPS5* (Figure 5B, compare region 8 between WT and *Δhmo1*). Because this region is occupied by PIC but not by Hmo1 in WT cells (Figure 5A), we assume that this slight increase in histone H3 binding in *Δhmo1* cells may be caused by a decrease in PIC binding. However, we currently cannot exclude the opposite possibility that the increase in histone H3 binding may cause an upstream shift of the PIC assembly site. In this case, *Δhmo1* would somehow allow invasion of the +1 nucleosome into the core promoter, pushing the PIC towards a more upstream site(s) (Figure 6D, *Δhmo1*).

While the finding that Hmo1 specifically binds to the NFR on Hmo1 target genes suggests that a nucleosome-free state is a pre-requisite for Hmo1 binding, we have not yet been able to identify specific *cis*-element(s) for Hmo1 binding in the mapping analysis, possibly because there are multiple binding sites for Hmo1 in *RPS5*-IVR. Although the IFHL motif and/or GGY(n) repeat were proposed as a binding site for Hmo1 by bioinformatic approaches (22,52), not all Hmo1-enriched RPG promoters contain these element(s) (our unpublished data). Furthermore, deletion of the IFHL motif reduced Hmo1 binding only modestly (22) (our unpublished data). Previously, Hmo1 was isolated in a yeast one-hybrid screen as a CAG repeat binding protein (53). Notably, the CAG repeat and IFHL motifs [or GGY(n) repeat] are GC-rich. In addition, the GC-content in the IVR of Hmo1-enriched RPGs (48.6%) is significantly higher, on average, than in Hmo1-limited RPG (36.1%) (our unpublished data). Therefore, we speculate that Hmo1 may recognize sequences with a relatively high GC-content, as represented by the IFHL motif within the NFR, and conversely that Hmo1 may be excluded from core promoter regions, which are very AT-rich. This speculation seems to be consistent with the results in Supplementary Figure S6C and D.

In previous studies, *spt* was identified as a suppressor of defects associated with insertions of the Ty1 transposon or δ sequence into the *HIS4* or *LYS2* promoters (54–56). Despite the lack of direct evidence, it is likely that relocation of the TSS from the Ty1 or δ sequence to the original *HIS4* or *LYS2* promoters is caused by a shift in the PIC assembly site in some *spt* mutants. It is possible that mutations in TBP (*SPT15*), SAGA (*SPT3, SPT7, SPT8* and *SPT20*) and Mediator (*SPT13*) might cause this phenotype through changes in the sequence specificity of PIC components, not due to the unmasking of the NFR. Notably, *SPT2* encodes a yeast HMG-like protein and participates in the repression of cryptic transcription in the coding region (57,58), showing similarities to Hmo1. However, it is likely that the *spt* phenotype is due to destabilization of nucleosomes in *spt2* cells (57), and such a defect has also been described in *spt6* and *spt16* cells (59). Similarly, mutations in histones (*SPT11* and *SPT12*) and in the transcriptional regulators of histone genes (*SPT1*, *SPT10* and *SPT21*) may produce the *spt* phenotype by a similar mechanism. In contrast, Hmo1 does not severely affect the position/stability of nucleosomes, but rather functions as if it replaces the function of nucleosome to inhibit the access of various transcription factors. Consistently, *Δhmo1* did not show the *spt* phenotype (our unpublished data). Considering these differences, we propose that Hmo1 is a novel type of transcription factor that directs PIC assembly to a physiologically relevant site by a novel mechanism.

Considering the fundamental importance of nucleosomal structures for cell growth, it is difficult to determine the specific roles of −1/+1 nucleosomes in PIC assembly. Nevertheless, the precise positioning of these nucleosomes suggests that they would determine the 5′- and 3′-boundaries, respectively, of the zone for PIC assembly (i.e. NFR). In a subset of RPG promoters, Hmo1 binds to a region that is usually occupied by the −1 nucleosome in other promoters, while *Δhmo1* allows invasion of PIC assembly in this region. These results indicate that Hmo1, instead of the −1 nucleosome, would determine the 5′-boundary of the zone for PIC assembly, at least in Hmo1-enriched RPG promoters, whereas the +1 nucleosome would still determine the 3′-boundary even in these promoters. To our knowledge, this is the first experimental evidence to show that there is indeed a 5′-boundary at the zone for PIC assembly and that the boundary is formed by a protein other than histones, at least in some promoters. Currently, PIC components are thought to bind to core promoters via the recognition of defined (or ill-defined) *cis*-elements and/or histone modifications of −1/+1 nucleosomes (49). In this context, the mechanism described above, by which certain factor(s) restrict the zone for PIC assembly, should provide an additional layer of specificity to the system, ensuring that PIC can be assembled only at a physiologically relevant site.

Besides a role in directing PIC assembly to an appropriate site, Hmo1 may also promote PIC assembly itself, since the binding of PIC components decreased significantly in *Δhmo1* cells (Figure 6B). In such a role, Hmo1

could facilitate PIC assembly by recruiting and/or stabilizing TFIID on its target promoters, as proposed for the −1 and +1 nucleosomes (49), either via direct interaction with TFIID subunits (23), or through Fhl1/Ifh1 coactivators (2,22). In fact, some yeast (Nhp6a/b) and human (HMGB1/2) HMGB proteins are known to activate transcription by stabilizing the TBP/TFIID–TFIIA promoter complex (60,61).

As another mechanism, Hmo1 might promote transcription by bending or looping a promoter DNA (62). A recent study, using cryo-electron microscopy, revealed that Rap1 on the UAS associates with TFIIA/TFIID at the core promoter, resulting in the looping-out of the region between the UAS and core promoter (i.e. IVR) (63). Intriguingly, the IVRs of Hmo1-enriched RPGs are significantly longer (approximately twice) than those of Hmo1-limited RPGs (22) (our unpublished data). Therefore, Hmo1 might promote and/or stabilize loop-formation, thereby helping Rap1 to affect TFIIA/TFIID efficiently from a distance in RPG promoters containing long IVR. Consistent with this, a TFIIA mutant, *toa1-2 (*K255A R257A K259A), which has defect in loop-formation (63) or in TFIIA–TFIID interaction (64), showed synthetic growth defects with *Δhmo1* (23). At present, although there is no evidence to show that Hmo1-mediated loop-formation occurs *in vivo*, DNA-looping mediated by Top2 and Hmo1 was proposed to prevent chromosome fragility of variously transcribed intergenic regions in S-phase (21).

In summary, we found that Hmo1 plays a novel role in transcription by forming the 5′-boundary (instead of −1 nucleosome on many other promoters) for the PIC assembly zone on a subset of RPG promoters. Intriguingly, Hmo1 binds to 35S rDNA but only to nucleosome-free (i.e. actively transcribed) repeats in this gene (26). These alternate localizations of Hmo1 and nucleosomes to both RPG and rDNA loci indicate that Hmo1 may have specialized functions that cannot be replaced by nucleosomes. An attractive hypothesis is that the novel function of Hmo1 may play an important role in the coordinated synthesis of RP and rRNA under various environmental conditions. Further studies will be required to define more precisely the roles of Hmo1 in transcription at these two loci.

SUPPLEMENTARY DATA

Supplementary Data are available at NAR Online.

ACKNOWLEDGEMENTS

We would like to thank Drs H. Iwasaki, T. Wada, M. Imashimizu and other members of our laboratory for advice and helpful discussions. We also thank Drs R. Young and F. Winston for supplying the yeast strains; S.W. Ki and K. Ohtsuki for making yeast strains and plasmids; H. Takahashi for making anti-Sua7 antibody; and H. Hirano for kindly allowing us to use the real-time PCR machine.

FUNDING

The 2009 Strategic Research Project (No. W2104) of Yokohama City University, Yokohama Academic Foundation, Japan Society for the Promotion of Science; the Ministry of Education, Culture, Sports, Science and Technology of Japan; CREST, Japan Science and Technology Corporation. Funding for open access charge: The Ministry of Education, Culture, Sports, Science and Technology of Japan.

Conflict of interest statement. None declared.

REFERENCES

1. Warner,J.R. (1999) The economics of ribosome biosynthesis in yeast. *Trends Biochem. Sci.*, **24**, 437–440.
2. Kasahara,K., Ohtsuki,K., Ki,S., Aoyama,K., Takahashi,H., Kobayashi,T., Shirahige,K. and Kokubo,T. (2007) Assembly of regulatory factors on rRNA and ribosomal protein genes in Saccharomyces cerevisiae. *Mol. Cell. Biol.*, **27**, 6686–6705.
3. Lieb,J.D., Liu,X., Botstein,D. and Brown,P.O. (2001) Promoter-specific binding of Rap1 revealed by genome-wide maps of protein-DNA association. *Nat. Genet.*, **28**, 327–334.
4. Garbett,K.A., Tripathi,M.K., Cencki,B., Layer,J.H. and Weil,P.A. (2007) Yeast TFIID serves as a coactivator for Rap1p by direct protein-protein interaction. *Mol. Cell. Biol.*, **27**, 297–311.
5. Reid,J.L., Iyer,V.R., Brown,P.O. and Struhl,K. (2000) Coordinate regulation of yeast ribosomal protein genes is associated with targeted recruitment of Esa1 histone acetylase. *Mol. Cell*, **6**, 1297–1307.
6. Pina,B., Fernandez-Larrea,J., Garcia-Reyero,N. and Idrissi,F.Z. (2003) The different (sur)faces of Rap1p. *Mol. Genet. Genomics*, **268**, 791–798.
7. Bernstein,B.E., Liu,C.L., Humphrey,E.L., Perlstein,E.O. and Schreiber,S.L. (2004) Global nucleosome occupancy in yeast. *Genome Biol.*, **5**, R62.
8. Yu,L. and Morse,R.H. (1999) Chromatin opening and transactivator potentiation by RAP1 in Saccharomyces cerevisiae. *Mol. Cell. Biol.*, **19**, 5279–5288.
9. Lascaris,R.F., Groot,E., Hoen,P.B., Mager,W.H. and Planta,R.J. (2000) Different roles for abf1p and a T-rich promoter element in nucleosome organization of the yeast RPS28A gene. *Nucleic Acids Res.*, **28**, 1390–1396.
10. Hartley,P.D. and Madhani,H.D. (2009) Mechanisms that specify promoter nucleosome location and identity. *Cell*, **137**, 445–458.
11. Wade,J.T., Hall,D.B. and Struhl,K. (2004) The transcription factor Ifh1 is a key regulator of yeast ribosomal protein genes. *Nature*, **432**, 1054–1058.
12. Schawalder,S.B., Kabani,M., Howald,I., Choudhury,U., Werner,M. and Shore,D. (2004) Growth-regulated recruitment of the essential yeast ribosomal protein gene activator Ifh1. *Nature*, **432**, 1058–1061.
13. Martin,D.E., Soulard,A. and Hall,M.N. (2004) TOR regulates ribosomal protein gene expression via PKA and the Forkhead transcription factor FHL1. *Cell*, **119**, 969–979.
14. Rudra,D., Zhao,Y. and Warner,J.R. (2005) Central role of Ifh1p-Fhl1p interaction in the synthesis of yeast ribosomal proteins. *EMBO J.*, **24**, 533–542.
15. Fingerman,I., Nagaraj,V., Norris,D. and Vershon,A.K. (2003) Sfp1 plays a key role in yeast ribosome biogenesis. *Eukaryot. Cell*, **2**, 1061–1068.
16. Jorgensen,P., Rupes,I., Sharom,J.R., Schneper,L., Broach,J.R. and Tyers,M. (2004) A dynamic transcriptional network communicates growth potential to ribosome synthesis and critical cell size. *Genes Dev.*, **18**, 2491–2505.
17. Marion,R.M., Regev,A., Segal,E., Barash,Y., Koller,D., Friedman,N. and O'Shea,E.K. (2004) Sfp1 is a stress- and nutrient-sensitive regulator of ribosomal protein gene expression. *Proc. Natl Acad. Sci. USA*, **101**, 14315–14322.

18. Gadal,O., Labarre,S., Boschiero,C. and Thuriaux,P. (2002) Hmo1, an HMG-box protein, belongs to the yeast ribosomal DNA transcription system. *EMBO J.*, **21**, 5498–5507.
19. Alekseev,S.Y., Kovaltsova,S.V., Fedorova,I.V., Gracheva,L.M., Evstukhina,T.A., Peshekhonov,V.T. and Korolev,V.G. (2002) HSM2 (HMO1) gene participates in mutagenesis control in yeast Saccharomyces cerevisiae. *DNA Repair*, **1**, 287–297.
20. Berger,A.B., Decourty,L., Badis,G., Nehrbass,U., Jacquier,A. and Gadal,O. (2007) Hmo1 is required for TOR-dependent regulation of ribosomal protein gene transcription. *Mol. Cell. Biol.*, **27**, 8015–8026.
21. Bermejo,R., Capra,T., Gonzalez-Huici,V., Fachinetti,D., Cocito,A., Natoli,G., Katou,Y., Mori,H., Kurokawa,K., Shirahige,K. *et al.* (2009) Genome-organizing factors Top2 and Hmo1 prevent chromosome fragility at sites of S phase transcription. *Cell*, **138**, 870–884.
22. Hall,D.B., Wade,J.T. and Struhl,K. (2006) An HMG protein, Hmo1, associates with promoters of many ribosomal protein genes and throughout the rRNA gene locus in Saccharomyces cerevisiae. *Mol. Cell. Biol.*, **26**, 3672–3679.
23. Kasahara,K., Ki,S., Aoyama,K., Takahashi,H. and Kokubo,T. (2008) Saccharomyces cerevisiae HMO1 interacts with TFIID and participates in start site selection by RNA polymerase II. *Nucleic Acids Res.*, **36**, 1343–1357.
24. Kim,H. and Livingston,D.M. (2009) Suppression of a DNA polymerase delta mutation by the absence of the high mobility group protein Hmo1 in Saccharomyces cerevisiae. *Curr. Genet.*, **55**, 127–138.
25. Lu,J., Kobayashi,R. and Brill,S.J. (1996) Characterization of a high mobility group 1/2 homolog in yeast. *J. Biol. Chem.*, **271**, 33678–33685.
26. Merz,K., Hondele,M., Goetze,H., Gmelch,K., Stoeckl,U. and Griesenbeck,J. (2008) Actively transcribed rRNA genes in S. cerevisiae are organized in a specialized chromatin associated with the high-mobility group protein Hmo1 and are largely devoid of histone molecules. *Genes Dev.*, **22**, 1190–1204.
27. Goetze,H., Wittner,M., Hamperl,S., Hondele,M., Merz,K., Stoeckl,U. and Griesenbeck,J. (2010) Alternative chromatin structures of the 35S rRNA genes in Saccharomyces cerevisiae provide a molecular basis for the selective recruitment of RNA polymerases I and II. *Mol. Cell. Biol.*, **30**, 2028–2045.
28. Goncalves,P.M., Griffioen,G., Minnee,R., Bosma,M., Kraakman,L.S., Mager,W.H. and Planta,R.J. (1995) Transcription activation of yeast ribosomal protein genes requires additional elements apart from binding sites for Abf1p or Rap1p. *Nucleic Acids Res.*, **23**, 1475–1480.
29. Mencia,M., Moqtaderi,Z., Geisberg,J.V., Kuras,L. and Struhl,K. (2002) Activator-specific recruitment of TFIID and regulation of ribosomal protein genes in yeast. *Mol. Cell*, **9**, 823–833.
30. Khaperskyy,D.A., Ammerman,M.L., Majovski,R.C. and Ponticelli,A.S. (2008) Functions of Saccharomyces cerevisiae TFIIF during transcription start site utilization. *Mol. Cell. Biol.*, **28**, 3757–3766.
31. Ghazy,M.A., Brodie,S.A., Ammerman,M.L., Ziegler,L.M. and Ponticelli,A.S. (2004) Amino acid substitutions in yeast TFIIF confer upstream shifts in transcription initiation and altered interaction with RNA polymerase II. *Mol. Cell. Biol.*, **24**, 10975–10985.
32. Freire-Picos,M.A., Krishnamurthy,S., Sun,Z.W. and Hampsey,M. (2005) Evidence that the Tfg1/Tfg2 dimer interface of TFIIF lies near the active center of the RNA polymerase II initiation complex. *Nucleic Acids Res.*, **33**, 5045–5052.
33. Sun,Z.W. and Hampsey,M. (1995) Identification of the gene (SSU71/TFG1) encoding the largest subunit of transcription factor TFIIF as a suppressor of a TFIIB mutation in Saccharomyces cerevisiae. *Proc. Natl Acad. Sci. USA.*, **92**, 3127–3131.
34. Chen,B.S. and Hampsey,M. (2004) Functional interaction between TFIIB and the Rpb2 subunit of RNA polymerase II: implications for the mechanism of transcription initiation. *Mol. Cell. Biol.*, **24**, 3983–3991.
35. Ziegler,L.M., Khaperskyy,D.A., Ammerman,M.L. and Ponticelli,A.S. (2003) Yeast RNA polymerase II lacking the Rpb9 subunit is impaired for interaction with transcription factor IIF. *J. Biol. Chem.*, **278**, 48950–48956.
36. Sun,Z.W., Tessmer,A. and Hampsey,M. (1996) Functional interaction between TFIIB and the Rpb9 (Ssu73) subunit of RNA polymerase II in Saccharomyces cerevisiae. *Nucleic Acids Res.*, **24**, 2560–2566.
37. Hull,M.W., McKune,K. and Woychik,N.A. (1995) RNA polymerase II subunit RPB9 is required for accurate start site selection. *Genes Dev.*, **9**, 481–490.
38. Chen,Z.A., Jawhari,A., Fischer,L., Buchen,C., Tahir,S., Kamenski,T., Rasmussen,M., Lariviere,L., Bukowski-Wills,J.C., Nilges,M. *et al.* (2010) Architecture of the RNA polymerase II-TFIIF complex revealed by cross-linking and mass spectrometry. *EMBO J.*, **29**, 717–726.
39. Eichner,J., Chen,H.T., Warfield,L. and Hahn,S. (2010) Position of the general transcription factor TFIIF within the RNA polymerase II transcription preinitiation complex. *EMBO J.*, **29**, 706–716.
40. Amberg,D.C., Burke,D.J. and Strathern,J.N. (2005) *Methods in Yeast Genetics: a Cold Spring Harbor Laboratory Course Manual.* Cold Spring Harbor Laboratory Press, Cold Spring Harbor, NY.
41. Kasahara,K., Kawaichi,M. and Kokubo,T. (2004) In vivo synthesis of Taf1p lacking the TAF N-terminal domain using alternative transcription or translation initiation sites. *Genes Cells*, **9**, 709–721.
42. Berroteran,R.W., Ware,D.E. and Hampsey,M. (1994) The sua8 suppressors of Saccharomyces cerevisiae encode replacements of conserved residues within the largest subunit of RNA polymerase II and affect transcription start site selection similarly to sua7 (TFIIB) mutations. *Mol. Cell. Biol.*, **14**, 226–237.
43. Majovski,R.C., Khaperskyy,D.A., Ghazy,M.A. and Ponticelli,A.S. (2005) A functional role for the switch 2 region of yeast RNA polymerase II in transcription start site utilization and abortive initiation. *J. Biol. Chem.*, **280**, 34917–34923.
44. Giardina,C. and Lis,J.T. (1993) DNA melting on yeast RNA polymerase II promoters. *Science*, **261**, 759–762.
45. Kuehner,J.N. and Brow,D.A. (2006) Quantitative analysis of in vivo initiator selection by yeast RNA polymerase II supports a scanning model. *J. Biol. Chem.*, **281**, 14119–14128.
46. Hampsey,M. (2006) The Pol II initiation complex: finding a place to start. *Nat. Struct. Mol. Biol.*, **13**, 564–566.
47. Tsukihashi,Y., Miyake,T., Kawaichi,M. and Kokubo,T. (2000) Impaired core promoter recognition caused by novel yeast TAF145 mutations can be restored by creating a canonical TATA element within the promoter region of the TUB2 gene. *Mol. Cell. Biol.*, **20**, 2385–2399.
48. Mavrich,T.N., Ioshikhes,I.P., Venters,B.J., Jiang,C., Tomsho,L.P., Qi,J., Schuster,S.C., Albert,I. and Pugh,B.F. (2008) A barrier nucleosome model for statistical positioning of nucleosomes throughout the yeast genome. *Genome Res.*, **18**, 1073–1083.
49. Jiang,C. and Pugh,B.F. (2009) Nucleosome positioning and gene regulation: advances through genomics. *Nat. Rev. Genet.*, **10**, 161–172.
50. Venters,B.J. and Pugh,B.F. (2009) How eukaryotic genes are transcribed. *Crit. Rev. Biochem. Mol. Biol.*, **44**, 117–141.
51. Sugihara,F., Kasahara,K. and Kokubo,T. (2010) Highly redundant function of multiple AT-rich sequences as core promoter elements in the TATA-less RPS5 promoter of Saccharomyces cerevisiae. *Nucleic Acids Res.*, **39**, 59–75.
52. Lavoie,H., Hogues,H., Mallick,J., Sellam,A., Nantel,A. and Whiteway,M. (2010) Evolutionary tinkering with conserved components of a transcriptional regulatory network. *PLoS Biol.*, **8**, e1000329.
53. Kim,H. and Livingston,D.M. (2006) A high mobility group protein binds to long CAG repeat tracts and establishes their chromatin organization in Saccharomyces cerevisiae. *J. Biol. Chem.*, **281**, 15735–15740.
54. Winston,F., Dollard,C., Malone,E.A., Clare,J., Kapakos,J.G., Farabaugh,P. and Minehart,P.L. (1987) Three genes are required for trans-activation of Ty transcription in yeast. *Genetics*, **115**, 649–656.
55. Winston,F., Chaleff,D.T., Valent,B. and Fink,G.R. (1984) Mutations affecting Ty-mediated expression of the HIS4 gene of Saccharomyces cerevisiae. *Genetics*, **107**, 179–197.

56. Fassler,J.S. and Winston,F. (1988) Isolation and analysis of a novel class of suppressor of Ty insertion mutations in Saccharomyces cerevisiae. *Genetics*, **118**, 203–212.
57. Nourani,A., Robert,F. and Winston,F. (2006) Evidence that Spt2/Sin1, an HMG-like factor, plays roles in transcription elongation, chromatin structure, and genome stability in Saccharomyces cerevisiae. *Mol. Cell. Biol.*, **26**, 1496–1509.
58. Cheung,V., Chua,G., Batada,N.N., Landry,C.R., Michnick,S.W., Hughes,T.R. and Winston,F. (2008) Chromatin- and transcription-related factors repress transcription from within coding regions throughout the Saccharomyces cerevisiae genome. *PLoS Biol.*, **6**, e277.
59. Belotserkovskaya,R. and Reinberg,D. (2004) Facts about FACT and transcript elongation through chromatin. *Curr. Opin. Genet. Dev.*, **14**, 139–146.
60. Shykind,B.M., Kim,J. and Sharp,P.A. (1995) Activation of the TFIID-TFIIA complex with HMG-2. *Genes Dev.*, **9**, 1354–1365.
61. Paull,T.T., Carey,M. and Johnson,R.C. (1996) Yeast HMG proteins NHP6A/B potentiate promoter-specific transcriptional activation in vivo and assembly of preinitiation complexes in vitro. *Genes Dev.*, **10**, 2769–2781.
62. Xiao,L., Williams,A.M. and Grove,A. (2010) The C-terminal domain of yeast high mobility group protein HMO1 mediates lateral protein accretion and in-phase DNA bending. *Biochemistry*, **49**, 4051–4059.
63. Papai,G., Tripathi,M.K., Ruhlmann,C., Layer,J.H., Weil,P.A. and Schultz,P. (2010) TFIIA and the transactivator Rap1 cooperate to commit TFIID for transcription initiation. *Nature*, **465**, 956–960.
64. Kang,J.J., Auble,D.T., Ranish,J.A. and Hahn,S. (1995) Analysis of the yeast transcription factor TFIIA: distinct functional regions and a polymerase II-specific role in basal and activated transcription. *Mol. Cell. Biol.*, **15**, 1234–1243.